

Solid-state lamps with optimized color saturation ability

Artūras Žukauskas,^{1*} Rimantas Vaicekuskas,² and Michael Shur³

¹Institute of Applied Research, Vilnius University, Saulėtekio al. 9-III, LT-10222 Vilnius, Lithuania

²Department of Computer Science, Vilnius University, Naugarduko 24, LT-03225 Vilnius, Lithuania

³Department of Electrical, Computer, and System Engineering, Rensselaer Polytechnic Institute, 110 8th Street, Troy, NY 12180, U.S.A.

*arturas.zukauskas@ff.vu.lt

Abstract: Spectral power distribution of trichromatic clusters of light-emitting diodes (LEDs) was optimized for rendering the highest number of colors with a perceptually noticeable gain in chroma (color saturation) out of 1269 Munsell samples. The basic tradeoffs of the number of colors rendered with increased saturation with the number of colors rendered with high fidelity and with luminous efficacy of radiation were established. High-saturation RGB clusters composed of commercially available AlGaInP and InGaN LEDs were modeled for a standard set of correlated color temperatures and the stability of the color saturation ability of the clusters against the drift of peak wavelengths was investigated.

©2010 Optical Society of America

OCIS codes: (330.1690) Color; (330.1715) Color, rendering and metamerism; (230.3670) Light emitting diodes.

References and links

1. Commission Internationale de l'Eclairage, "Method of measuring and specifying colour rendering properties of light sources," Pub. CIE 13.3, 1995.
2. Commission Internationale de l'Eclairage, "Colour rendering of white LED sources," Pub. CIE 177, 2007.
3. W. Davis, and Y. Ohno, "Toward and improved color rendering metrics," Proc. SPIE **5941**, 59411G1–8 (2005).
4. D. B. Judd, "A flattery index for artificial illuminants," Illum. Eng. **62**, 593–598 (1967).
5. W. A. Thornton, "Color-discrimination index," J. Opt. Soc. Am. **62**(2), 191–194 (1972).
6. W. A. Thornton, "A validation of the color-preference index," J. Illum. Eng. Soc. **4**, 48–52 (1974).
7. S. M. Aston, and H. E. Belchambers, "Illumination, color rendering, and visual clarity," Lighting Res. Tech. **1**(4), 259–261 (1969).
8. K. Hashimoto, and Y. Nayatani, "Visual clarity and feeling of contrast," Color Res. Appl. **19**(3), 171–185 (1994).
9. H. Xu, "Color-rendering capacity of illumination," J. Opt. Soc. Am. **73**(12), 1709–1713 (1983).
10. Y. Nakano, H. Tahara, H. Suehara, J. Kohda, and T. Yano, "Application of multispectral camera to color rendering simulator," in *Proceedings of AIC Colour 05 – 10th Congress of the International Colour Association* (Granada, Spain, 2005), pp. 1625–1628.
11. K. Hashimoto, T. Yano, M. Shimizu, and Y. Nayatani, "New method for specifying color-rendering properties of light sources based of feeling of contrast," Color Res. Appl. **32**(5), 361–371 (2007).
12. M. S. Rea, and J. P. Freyssinier-Nova, "Color rendering: A tale of two metrics," Color Res. Appl. **33**(3), 192–202 (2008).
13. A. Žukauskas, R. Vaicekuskas, F. Ivanauskas, H. Vaitkevičius, P. Vitta, and M. S. Shur, "Statistical approach to color quality of solid-state lamps," IEEE J. Sel. Top. Quantum Electron. **15**(6), 1753–1762 (2009).
14. A. Žukauskas, M. S. Shur, and R. Gaska, *Introduction to Solid-State Lighting* (Wiley, New York, 2002).
15. D. A. Steigerwald, J. C. Bhat, D. Collins, R. M. Fletcher, M. O. Holcomb, M. J. Ludowise, P. S. Martin, and S. L. Rudaz, "Illumination with solid state lighting technology," IEEE J. Sel. Top. Quantum Electron. **8**(2), 310–320 (2002).
16. M. Shur, and A. Žukauskas, "Solid-state lighting: Toward superior illumination," Proc. IEEE **93**(10), 1691–1703 (2005).
17. E. F. Schubert, and J. K. Kim, "Solid-state light sources getting smart," Science **308**(5726), 1274–1278 (2005).
18. P. J. Bouma, "The colour reproduction of incandescent lamps and 'Philiphpan' glass," Philips', Technol. Rev. **3**, 47–49 (1938).
19. J. J. McCann, S. P. McKee, and T. H. Taylor, "Quantitative studies in retinex theory. A comparison between theoretical predictions and observer responses to the "color mondrian" experiments," Vision Res. **16**(5), 445–458 (1976).
20. J. A. Worthey, "Color rendering: Asking the question," Color Res. Appl. **28**(6), 403–412 (2003).
21. N. Narendran, and L. Deng, "Color rendering properties of LED sources," Proc. SPIE **4776**, 61–67 (2002).

22. Y. Ohno, "Spectral design considerations for white LED color rendering," *Opt. Eng.* **44**(11), 111302 (2005).
 23. Spectral Database, University of Joensuu Color Group., Available: <http://spectral.joensuu.fi/>.
 24. D. L. MacAdam, "Visual sensitivities to color differences in daylight," *J. Opt. Soc. Am.* **32**(5), 247–274 (1942).
 25. *Specifications for the Chromaticity of Solid State Lighting Products*, ANSI Standard C78.377–2008.
 26. G. Wyszecki, and W. S. Stiles, *Color Science. Concepts and Methods, Quantitative Data and Formulae*, (Wiley, New York, 2000).
 27. A. Žukauskas, R. Vaicekauskas, F. Ivanauskas, R. Gaska, and M. S. Shur, "Optimization of white polychromatic semiconductor lamps," *Appl. Phys. Lett.* **80**(2), 234–236 (2002).
 28. A. Žukauskas, R. Vaicekauskas, F. Ivanauskas, H. Vaitkevičius, and M. S. Shur, "Rendering a color palette by light-emitting diodes," *Appl. Phys. Lett.* **93**(2), 021109 (2008).
 29. A. Žukauskas, F. Ivanauskas, R. Vaicekauskas, M. S. Shur, and R. Gaska, "Optimization of multichip white solid-state lighting source with four or more LEDs," *Proc. SPIE* **4445**, 148–155 (2001).
-

1. Introduction

Until recently, a sole accepted characteristic of quality of a white lighting source was its ability to reproduce colors of the illuminated objects with high fidelity, i.e. as close as possible to those perceived under sunlight or blackbody radiators. This ability is measured by a widely recognized figure of merit, the general color rendering index (R_a) introduced by the CIE (Commission Internationale de l'Éclairage) [1] and presently being subjected to some criticism [2] and refinement [3]. Another important qualitative characteristic of lighting, which is its ability to make colors vivid and easily distinguishable (basically due to rendering surface colors with increased saturation rather than with high fidelity), received less attention from industry, due mainly to the lack of technological means to control this characteristic. Nevertheless, this second aspect of quality of lighting has been widely discussed within the scientific community using numerous mutually interrelated approaches, such as flattery index [4], color-discrimination index [5], color-preference index [6], visual clarity approach [7,8], color-rendering capacity [9], impression of colorfulness [10], index on feeling of contrast [11], gamut-area index [12], and color saturation index [13]. Light sources that provide improved color discrimination ability can find numerous applications in performing specific visual tasks, as well as in commercial, architectural, and entertainment lighting. Recently such sources became more feasible due to advancements in solid-state lighting technology, which offers unexcelled possibilities in tailoring the illumination spectrum through generation of narrow-band emission in different semiconductor junctions and wavelength conversion in phosphors [14–17].

Effect of increased color saturation by removing the yellow component from the emission spectrum of incandescent lamps by a neodymium glass filter is known for years [18]. Also, it is known that a source of white light composed of three narrow-band red (R), green (G), and blue (B) emitters with the spectral peaks at, e.g., 630, 530, and 450 nm, respectively, makes surface colors appear more saturated than under a broad-band illuminant [19]. The reason is in that in both cases, chromaticity coordinates of many color samples shift toward increased chroma [20]. Recently, this effect received attention when designing light-emitting diode (LED) based trichromatic sources of light with tailored color rendering characteristics. In particular, human subject response for color preference of objects illuminated by trichromatic LED clusters was found to be higher than that of objects illuminated by incandescent lamps and phosphor-conversion LEDs having larger values of R_a [21]. Also, application of the semantic differential method for several combinations of commercial LEDs revealed that the visual impression of colorfulness of the illuminated natural scenes was higher, when spectral power distribution of the illuminants had a strong component in the region of wavelengths longer than 600 nm [10]. Other approaches confirmed that the peak wavelength of the longest-wavelength LED in RGB clusters strongly influences the feeling of contrast [11] and the number of colors rendered with increased saturation [13]. Another example is an enhanced chroma for most of 14 CIE standard test color samples under illumination by an RGB cluster composed of 455-nm, 547-nm, and 623-nm LEDs [22]. However despite some demonstrative examples, no general design rules for solid-state sources of light, which can increase colorfulness of the illuminated objects to a maximal extent, have been developed so far.

In this work, we present the results of optimization of the spectral power distribution (SPD) of trichromatic LED-based sources of white light with high color saturation ability. Our approach is based on maximizing the color saturation index (CSI), a figure of merit recently introduced for rating of color rendering properties of solid-state lamps [13]. In contrast to the previous approaches [4–12], CSI is a statistical approach, which allows to computationally quantify the color saturation effect for a very large number of test color samples, including those with highly saturated colors.

2. Optimization model

The principle criterion of optimization used in our approach is CSI, a relative number (percentage) of test color samples out of a large set that gain a perceptually noticeable increase in chroma when a reference illuminant is replaced by a source under test [13]. The set of test color samples used is a spectrophotometrically calibrated palette of 1269 Munsell samples [23]. A perceptually noticeable gain in chroma is recorded when the projection of the color-shift vector onto the saturation (chroma) direction within a color space escapes from the 3-step MacAdam ellipse centered at the chromaticity coordinates of the sample. Within such an approach, the value of CSI is invariant in respect of the color space used. A set of 1269 MacAdam ellipses was obtained by interpolation of the original MacAdam data for 25 colors [24]. The statistical format of the index allows using a large number of test color samples and collating the magnitude of CSI with that of other indices estimated in the same format, such as color fidelity index (CFI, the percentage of samples with no perceptually noticeable color shift) and hue distortion index (HDI, the percentage of samples with a perceptually noticeable change in hue) [13]. Here we use two additional optimization criteria that are in a tradeoff with CSI. These are either CFI or luminous efficacy of radiation (LER). The latter is the luminous flux per unit radiant flux for a given SPD, $S(\lambda)$,

$$\text{LER} = 683 \text{ lm/W} \times \int_{380 \text{ nm}}^{780 \text{ nm}} S(\lambda) V(\lambda) d\lambda \bigg/ \int_0^{\infty} S(\lambda) d\lambda, \quad (1)$$

where $V(\lambda)$ is the 1924 CIE spectral luminous efficiency function. The goal of the optimization problem is finding SPDs for lamps, which render more colors with increased chroma than with high fidelity ($\text{CSI} > \text{CFI}$), and have both high CSI and LER. The reference illuminants used here are the blackbody illuminant with the correlated color temperature (CCT) of 3000 K for warm white lamps and the daylight phase illuminant (CCT = 6500 K) for daylight lamps [25].

Consider SPDs due to n colored primary LEDs each emitting within a narrow band of a particular shape. Each SPD is characterized by a vector in the $2n$ -dimensional parametric space $\{\lambda_1, \dots, \lambda_n, \Phi_1, \dots, \Phi_n\}$ of peak wavelengths λ_i and fractional radiant fluxes Φ_i that are subjected to three constraints that follow from three common color-mixing equations [26]. This parametric space with $2n-3$ degrees of freedom is the optimization domain where an objective function is maximized [27]. Note that under dichromatic blends of narrow-band emissions the contrast for most surface colors is lost [20], whereas tetrachromatic and higher blends render colors with high fidelity rather than with increased saturation [13,28]. Therefore, only trichromatic blends were considered ($n = 3$). The objective function maximized is a weighted sum of CSI and a parameter P , which CSI is considered to be in a tradeoff with,

$$F_{\sigma}(\lambda_1, \lambda_2, \lambda_3, \Phi_1, \Phi_2, \Phi_3) = \sigma \times \text{CSI} + (1 - \sigma)P, \quad (2)$$

where σ is the weight that controls the tradeoff ($0 \leq \sigma \leq 1$). As indicated above, the trade-off parameter, P , considered here is either CFI or LER.

For $n = 3$, the optimization problem can be solved by searching inside the 3-dimensional parametric space of peak wavelengths (fractional radiant fluxes are found from the three color-mixing equations). Through the calculation of CSI and P for each set of wavelengths, a

phase distribution (CSI, P) is generated and the optimal (upper-right) boundary of the distribution (Pareto boundary) can be found. The Pareto boundary corresponds to the maximized target function with the weight parameter spanning over the interval (0,1). In other words, the end points of the boundary correspond to the highest CSI and P , respectively, whereas the points in between them show all possible optimal tradeoffs.

The optimization results presented in Section 3 involve SPDs composed of three LED lines approximated by Gaussian shapes with equal full width at half magnitude (FWHM, Δ) of the LED emission band. Practical high-saturation lamps were modeled using actual emission spectra of commercially available AlGaInP and InGaN LEDs (Section 4). All considered SPDs had chromaticity coordinates equal to those of the relevant reference illuminant in order to avoid chromatic adaptation issues.

3. Results of optimization

The light sources that have SPDs composed of three narrow bands are able of exhibiting color saturation effect [13,19,20]. In order to evaluate the feasibility of LEDs for designing sources of light with high color saturation ability, we first examined a dependence of the color quality indices on the bandwidth of the primary emissions with Gaussian SPDs. Figure 1 shows the statistical color quality indices (CSI, CFI, and HDI) as well as LER as functions of FWHM for the known set of peak wavelengths of 630 nm, 530 nm, 450 nm [19] at the two CCTs. At low values of bandwidth ($\Delta < 20$ nm), the color saturation effect is almost constant with the CSI of 82% and 71% for warm white and daylight illuminant, respectively, with CFI being below 10%, and HDI of 75% and 67%, respectively. (For comparison, the estimated values of CSI, CFI, and HDI for an incandescent lamp with a neodymium glass filter [18,22] are 52%, 37%, and 15%, respectively.) CSI drops by about 5% at a ~35-nm FWHM and, at about 70-nm FWHM, CSI and CFI have already equal values of about 40%. With further increasing of the bandwidth up to 100 nm, CSI drops to marginal values and CFI exceeds 90%. The hue distortion index is in correlation with CSI (decreases with FWHM). LER has the highest values at small FWHMs (295 lm/W and 286 lm/W for CCT of 3000 K and 6500 K, respectively) and decreases to 283 lm/W and 250 lm/W, respectively, at a 100-nm bandwidth.

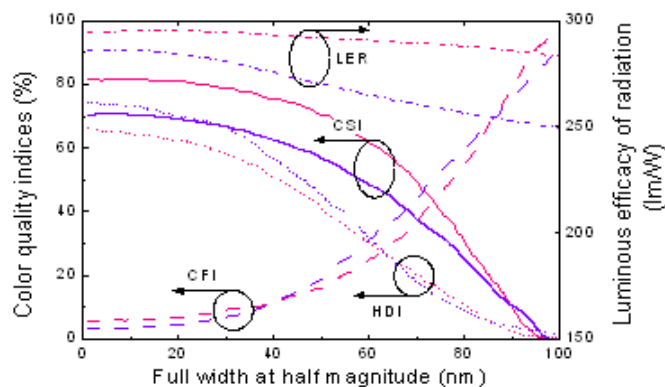


Fig. 1. Color-quality indices of trichromatic sources of light as functions of bandwidth (FWHM) of the primary emissions with the peak wavelengths of 630 nm, 530 nm, and 450 nm. Solid lines, color saturation index (CSI); dashed lines, color fidelity index (CFI); dotted lines, hue distortion index (HDI); dash-dotted lines, luminous efficacy of radiation (LER). Pink lines, CCT = 3000 K; violet lines, CCT = 6500 K.

The results shown in Fig. 1 demonstrate that colored inorganic-semiconductor junction LEDs are good candidates for the development of trichromatic lamps with high color saturation ability. For example, common red to amber AlGaInP LEDs have FWHMs in the range of 15 to 30 nm depending on the wavelength and operating junction temperature, whereas green to blue InGaN LEDs have bandwidths in the range of 20 to 50 nm. Typically, an RGB cluster requires one AlGaInP LED and two InGaN LEDs with the FWHM averaged

over those three of about 30 nm, and we use this bandwidth for the establishment of basic optimization tradeoffs between CSI and either LER or CFI. Although a larger average FWHM generally results in a drop of CSI, the effect of increased FWHM of individual LEDs on CSI depends on the peak wavelength and fractional radiant flux (see discussion in Section 4).

Figure 2a shows the result of the optimal tradeoff between CSI and LER (Pareto boundaries) for 30-nm LED bandwidths and Fig. 2b displays the corresponding peak wavelengths of the primary emissions. The highest values of CSI are seen to be attained at nearly zero LER, since the red and blue peaks reside at the edges of the visible spectrum. However, LER can be substantially increased up to ~300 lm/W and ~250 lm/W for CCT of 3000 K and 6500 K, respectively, by shifting the red and blue components toward the centre of the spectrum (to about 625 nm and 440 nm, respectively) at a very small expense of CSI. From the point of view of higher efficacy, an important part of the tradeoff is in the LER intervals of 300 to 380 lm/W and 250 to 320 lm/W for CCT of 3000 K and 6500 K, respectively, where CSI is still high (drops from about 80% to about 60%). In these intervals, the blue component maintains almost constant position around 450 nm, whereas the green and red components approach each other by moving from 520 to ~530 nm and from 625 to 612 nm, respectively. This means that efficient RGB clusters with high color saturation ability must be composed of blue LEDs emitting at about 450 nm and of green and red LEDs with the peak wavelengths residing within the 520–530 nm and 612–625 nm ranges, respectively.

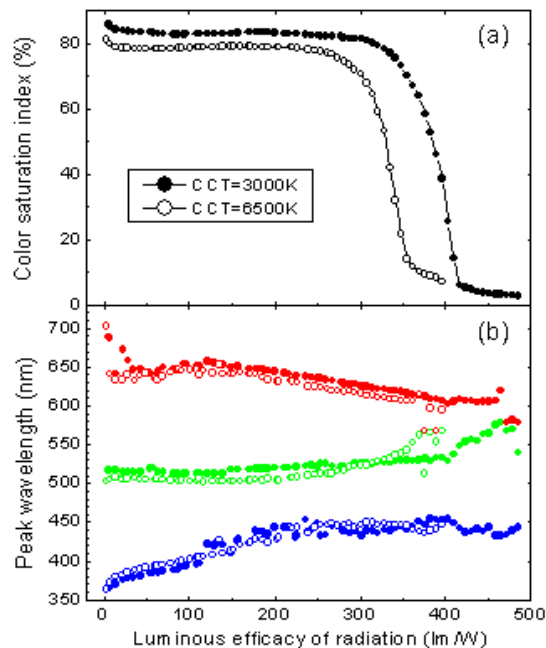


Fig. 2. (a) Maximized color saturation index as a function of luminous efficacy of radiation (LER) for a trichromatic illuminant with the bandwidth of the primary emissions of 30 nm. (b) Peak wavelengths of the primary emissions as functions of LER. Solid points, CCT = 3000 K; open points, CCT = 6500 K.

With a further LER increase, the maximized CSI exhibits an abrupt drop to marginal values of 3 to 10% (Fig. 2a). The lowest values of CSI and the highest values of LER are attained when the red and green lines merge and the trichromatic RGB cluster converts to a dichromatic yellow-blue one.

Figure 3a shows the Pareto boundaries of the tradeoff between CSI and CFI for 30-nm LED bandwidths. Figure 3b displays the corresponding peak wavelengths of the primary emissions. The results are very similar for both values of CCT, with somewhat higher values of CSI at 3000 K. CSI and CFI are seen to be in an almost linear negative tradeoff, i. e. an

increase in CFI is gained at the same expense of CSI. The highest values of CSI at about 80% are attained at almost zero CFI with the same SPDs as those for highest CSIs and zero LER in Fig. 2. Again, CSI can be preserved in excess of 60% with low CFI values (5–20%) when the red and blue components are shifted toward the centre of the spectrum for increased efficacy. For the CSI values at about 70%, the wavelength ranges for the blue, green, and red LEDs are very similar to the optimal ones that were defined through the CSI–LER tradeoff, i. e. efficient RGB clusters with high color saturation ability are to be composed of blue, green, and red LEDs with the peak wavelengths around 450 nm, 525 nm, and 630 nm, respectively. However, the results presented in Fig. 3 indicate that the tradeoff between CSI and CFI is rather sensitive to the peak wavelengths of the primary LEDs. For instance, when the peaks move to 465 nm, 530 nm, and 606 nm, CFI catches up with CSI at about 40% and the number of colors rendered with high fidelity starts exceeding that of colors rendered with increased saturation. This poses a potential problem of stability of high-saturation RGB clusters with respect to technological scatter and thermal drifts of the peak wavelengths (see Section 4 for a specific example).

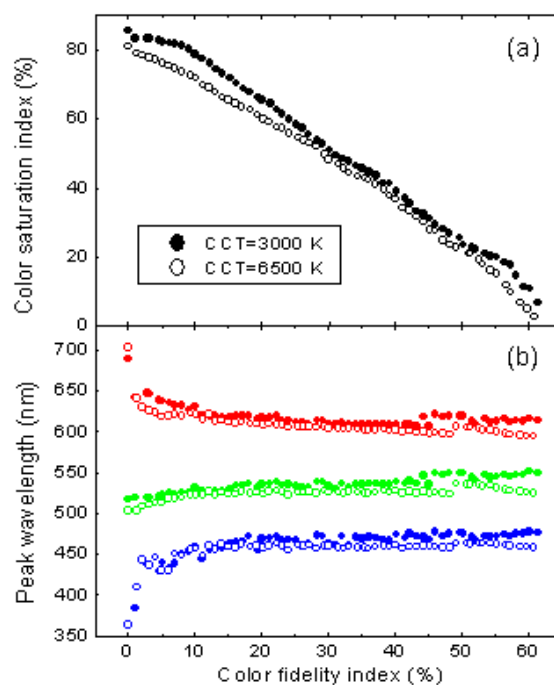


Fig. 3. (a) Maximized color saturation index as a function of color fidelity index (CFI) for a trichromatic illuminant with the bandwidth (FWHM) of primary emissions of 30 nm. (b) Peak wavelengths of the primary emissions as functions of CFI. Solid points, CCT = 3000 K; open points, CCT = 6500 K.

The above optimization results obtained within a rigorous and systematic approach account for previous empirical findings in composing a spectrum of sources of light with an ability to saturate colors of illuminated objects. In particular, the obtained optimal peak wavelengths of the LEDs are very similar to those established empirically for the trichromatic source composed of narrow-band emissions (630 nm, 530 nm, and 450 nm) that makes surface colors appear more saturated [18]. Also, our results are in agreement with the SPDs of trichromatic LED clusters that render colors of objects illuminated with high subjective preferences [10,21].

4. High-saturation RGB clusters composed of commercially available LEDs

In the previous section, we established the optimal ranges of LED peak wavelengths and basic tradeoffs for color saturation ability versus color fidelity ability and versus efficacy for high-saturation trichromatic clusters with the LED spectra approximated by 30-nm wide Gaussian shapes. However, mass-produced commercial colored LEDs are available only for certain peak wavelengths that meet the needs of display and signage industries. Also, the actual shape of the emission bands is somewhat different from the Gaussian and LEDs of different colors have different bandwidths. Therefore, it is important to examine the feasibility of designing high-saturation RGB clusters using commercially available LEDs and to consider the aforementioned effect of possible technological scatter and thermal drift of the peak wavelengths on the color saturation ability.

As a model set of LEDs, Philips Lumileds Lighting Luxeon™ high-power (1 W) LED family was selected. The SPDs of cluster illuminants were simulated using the measured spectra of LEDs specified in the datasheets as red (spectral peak at 627 nm), red-orange (627 nm), amber (594 nm), green (519 nm), cyan (506 nm), blue (464 nm), and royal blue (442 nm). The spectra were measured at a nominal forward current (350 mA) when the temperature of the metal mount holding the chip was maintained at 25 °C.

Examination of all possible trichromatic compositions has shown that high color saturation indexes ($\geq 70\%$) can be obtained in eight types of clusters with the long-wavelength LED selected out of red or red-range ones, the medium-wavelength LED selected out of green or cyan ones, and the short-wavelength LED selected out of blue or royal blue ones. Below, we present the results on the modeling of a trichromatic cluster composed of 627-nm, 519-nm, and 442-nm LEDs thereafter designated as red, green, and blue LEDs, respectively. Out of the eight cluster types, this one has the highest LER and the highest product of LER and CSI for the entire CCT range.

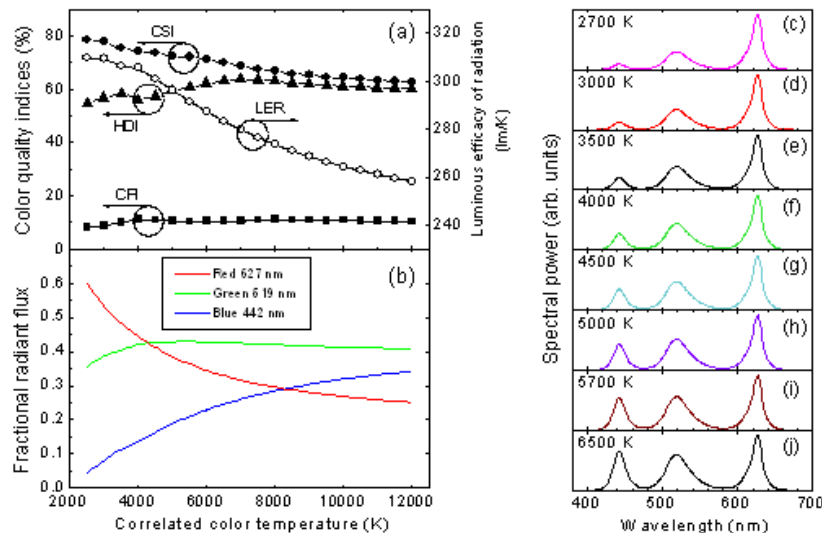


Fig. 4. (a) Color quality indices (filled points) and luminous efficacy of radiation (open points) of a trichromatic cluster composed of commercially available red 627-nm, green 519-nm, and blue 442-nm LEDs as functions of correlated color temperature (CCT). (b) Fractional radiant fluxes of the primary LEDs as functions of CCT. (c)–(j) Spectral power distributions of the trichromatic cluster for a set of CCTs specified by the ANSI standard [25].

Figure 4a shows color quality indices of the RGB trichromatic cluster composed of the selected red, green, and blue LED as functions of CCT. With increasing CCT from 2500 K to 12,500 K, CSI decreases from 78% to 62% but is still close to maximal possible values at reasonable LERs (see Figs. 2 and 3). In the same range, CFI exhibits only a small increase

from 8% to 10% what means that the number of colors rendered with high fidelity is much smaller than the number of those rendered with an increased saturation. Note that the percentage of colors rendered with distorted hue is rather high (HDI varies from 55% to 60%). Increasing CCT also results in the net LER decrease from 310 lm/W to 258 lm/W due to increasing contribution of the blue component, which has the lowest individual LER of the three ones. Figure 4b shows the fractional radiant fluxes of the red, green and blue LEDs as functions of CCT.

Table 1 presents numerical data on the parameters of the 627-519-442-nm LED cluster for eight CCTs specified by the ANSI for solid-state sources of light [25]. The eight emission spectra of the cluster are shown in Figs.4c–4j.

Table 1. Parameters of high-saturation RGB clusters composed of commercially available LEDs

CCT (K)	Color quality indices (%)			LER (lm/W)	R_a	Fractional radiant fluxes of the LEDs		
	CSI	CFI	HDI			442 nm	519 nm	627 nm
2700	78	8	56	310	34	0.060	0.370	0.570
3000	78	9	57	309	35	0.080	0.387	0.533
3500	75	10	58	306	37	0.113	0.404	0.483
4000	74	11	56	305	41	0.136	0.420	0.444
4500	74	11	57	301	43	0.163	0.426	0.411
5000	72	10	60	296	44	0.188	0.428	0.384
5700	71	10	62	290	46	0.218	0.428	0.354
6500	70	10	63	283	48	0.246	0.426	0.328

The luminous efficiency of an RGB LED cluster can be estimated as [29]

$$\eta_o = \text{LER} \times \sum_{i=1}^3 \Phi_i / \sum_{i=1}^3 \Phi_i / \eta_{ei}, \quad (3)$$

where η_{ei} are the radiant efficiencies of the individual LEDs.

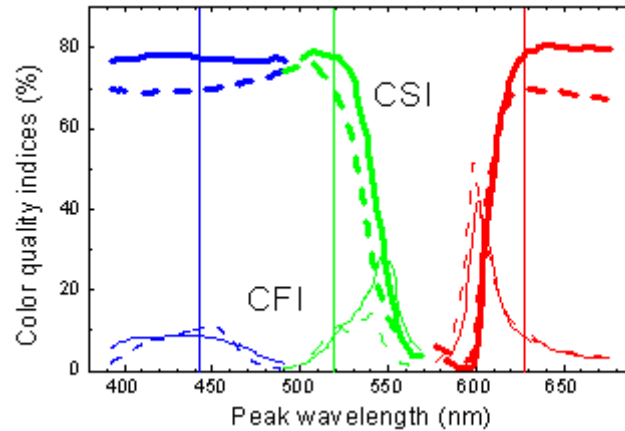


Fig. 5. Effect of shifting the peak wavelength on color quality of trichromatic LED clusters composed of commercially available red, green, and blue LEDs (vertical lines designate the initial peak wavelengths of 627 nm, 519 nm, and 442 nm, respectively). Bold lines, color saturation index; thin lines, color fidelity index. Solid and dashed lines stand for correlated color temperature of 3000 K and 6500 K, respectively.

Figure 5 presents data on the stability of the color-saturation ability of the designed RGB LED cluster with respect of possible scatter and thermal drift of the peak wavelengths. The bold lines in Fig. 5 show the variation of CSI of the cluster with shifting one of the three peaks when the remaining two being kept at the nominal position (with the partial radiant fluxes

synchronously adjusted to maintain the color point). The color saturation ability is rather insensitive to the blue LED drift for both examined CCTs (3000 K and 6500 K). However, CSI considerably drops with increasing the wavelength of the green LED and with decreasing the wavelength of the red LED by more than 10 nm. Simultaneously, CFI increases and reaches maximal values for the peak wavelengths of 540-550 nm and ~600 nm, respectively. Such instability might be marginal with respect to typical technological scatter of 2-3 nm. For typical temperature coefficients of the peak wavelengths of 0.05 nm/K and 0.13 nm/K for nitride green and phosphide red LEDs, respectively, a noticeable decrease in color saturation ability is also unlikely within the entire range of operating temperatures.

The data shown in Fig. 5 also indicate that the emission spectrum range between 530 nm and 610 nm has to be avoided for trichromatic lamps with high color saturation ability. (This is in agreement with the use of the incandescent lamps filtered by a neodymium glass [18].) Our analysis also shows that the yellow gap has different sensitivity to the bandwidth of different LEDs. First, an increase in the red and green LED bandwidth may result in an encroachment on the gap and therefore has a higher impact on the drop of CSI, whereas the FWHM of the blue LED has a marginal effect on the color saturation ability of the cluster. Second, the yellow gap is somewhat smeared when CCT is increased by relative increasing of the fractional radiant flux of the broader-band green LED with respect to that of the narrower-band red LED (see Figs. 4c-4j). This partially accounts for lower CSI values for clusters with higher CCTs (Table 1 and Fig. 4a).

5. Summary

In conclusion, colored LEDs were shown to have sufficiently narrow emission bands for composing them into trichromatic lighting clusters with a high ability of saturation of surface colors. However differently from the LED clusters that render colors with high fidelity [28], maximizing the color saturation ability through tailoring the LED peak wavelengths results in an unreasonably low efficacy. Also, relatively small variations in the peak wavelengths of the LEDs can result in an increase of the color fidelity ability at an expense of the color saturation ability. Therefore optimal tradeoffs of the color saturation index versus LER as well as CFI have been established. LED clusters with reasonable LERs were shown to be able to render more than 70% colors of the Munsell palette with increased chroma (color saturation). Commercially available red, green, and blue LEDs meet the requirements for the peak wavelengths of the RGB clusters with high color saturation ability. The SPDs of such clusters were demonstrated and the clusters were shown to have sufficient stability against technological scatter and thermal drift of the peak wavelengths provided that the yellow gap (between 530 nm and 610 nm) is kept unimpaired.

Acknowledgment

The work at RPI was partially supported by the National Science Foundation (NSF) Smart Lighting Engineering Research Center (# EEC-0812056).